



Title	Simplified parametric models of the dielectric properties of brain and muscle tissue during electrical stimulation
Authors(s)	Grant, Peadar F., Lowery, Madeleine M.
Publication date	2019-03
Publication information	Grant, Peadar F., and Madeleine M. Lowery. "Simplified Parametric Models of the Dielectric Properties of Brain and Muscle Tissue during Electrical Stimulation." Elsevier, March 2019. https://doi.org/10.1016/j.medengphy.2018.12.018 .
Publisher	Elsevier
Item record/more information	http://hdl.handle.net/10197/26553
Publisher's statement	This is the author's version of a work that was accepted for publication in Medical Engineering and Physics. Changes resulting from the publishing process, such as peer review, editing, corrections, structural formatting, and other quality control mechanisms may not be reflected in this document. Changes may have been made to this work since it was submitted for publication. A definitive version was subsequently published in Medical Engineering and Physics (65, pp. 61-67 (2019)) https://doi.org/10.1016/j.medengphy.2018.12.018
Publisher's version (DOI)	10.1016/j.medengphy.2018.12.018

Downloaded 2026-05-02 00:24:12

The UCD community has made this article openly available. Please share how this access benefits you. Your story matters! (@ucd_oa)



© Some rights reserved. For more information

1 Simplified parametric models of the dielectric properties of brain and 2 muscle tissue during electrical stimulation

3 Peadar F. Grant* and Madeleine M. Lowery†

4 March 16, 2018

5 Abstract

6 Parametric models are commonly used to describe the dispersive dielectric properties of biological tissues. While
7 distinct regions of dispersion have been identified, the relative contribution of each during electrical stimulation is un-
8 known. This study quantified the contribution of individual poles in parametric models of brain and muscle dielectric
9 properties during electrical stimulation. The effect on the extracellular voltage waveform and threshold current for nerve
10 stimulation of selectively removing subsets of poles from Cole-Cole and Debye models was examined. Errors were intro-
11 duced when dispersions below 100 kHz were removed in both brain and muscle tissue. Poles below 1 kHz influenced the
12 amplitude of the extracellular voltage waveform and the predicted minimum stimulation current. Poles between 1 kHz
13 and 100 kHz influenced the waveform shape, with a minor effect on stimulus amplitude. The results confirm that low
14 frequency dispersion in conductivity and permittivity can fundamentally influence the electric field and neural response
15 during stimulation and provide insight into the relative contribution of the different dispersive regimes. Furthermore, they
16 provide justification for for simplifying parametric models of dielectric properties through the removal of high frequency
17 poles above 100 kHz which could improve the efficiency of time-domain solvers for simulations involving time-varying
18 or aperiodic stimuli as may be required for certain closed-loop stimulation paradigms.

19 Keywords

20 electrical neural stimulation, dispersion, Cole-Cole model, Debye model, computational model

21 Word count

22 4165 excluding bibliography

*Department of Computing Science and Mathematics, School of Informatics and Creative Arts, Dundalk Institute of Technology, Dundalk, Co. Louth, Ireland, <peadar.grant@dkit.ie> [corresponding author, Rev ID: cfce5ec]

†UCD School of Electrical and Electronic Engineering, University College Dublin, Belfield, Dublin 4, Ireland.

23 1 Introduction

24 Modeling the electric field induced during electrical stimulation is a vital component in understanding how electrical
25 stimulation of nerves can modulate activity of the nervous system. Over the past several decades, it has provided insight
26 into the various effects of electrode geometry, tissue electrical properties and neural response across a range of application
27 areas. In the majority of modelling studies both to assess the efficacy of electrical stimulation and to simulate bioelectric
28 signals, it is assumed that capacitive, inductive and propagation effects can be neglected [1], a simplification known as
29 the quasi-static approximation [1–3]. Although inductive and propagation effects have been confirmed to be negligible
30 for frequencies and volume conductor dimensions of interest [2], analytical and simulation studies have suggested that
31 capacitive effects are the weakest of these three assumptions [2, 4–6]. In the case of deep brain stimulation using chroni-
32 cally implanted electrodes, incorporation of tissue capacitance into models of the electric field has been shown to increase
33 the minimum current required for axonal stimulation and reduce the estimated volume of excitable tissue activated by the
34 stimulus [6–8].

35 Additionally, the electrical conductivities and permittivities of many biological tissues are known to vary as a function
36 of excitation frequency [9–13]. Recent computational studies have shown that incorporating dielectric dispersion can
37 influence the thresholds for neural stimulation and has the greatest effect under current controlled stimulation or voltage
38 controlled stimulation when highly resistive encapsulation tissue surrounds the electrode [7, 14], but has limited effect
39 when no encapsulation tissue is present. Simulation studies have reported that frequency-independent resistive and capac-
40 itive approximations of the fully dispersive tissue model may provide accurate estimates of stimulation efficacy, subject
41 to the properties’ being estimated at an appropriate frequency [2, 7].

42 Dielectric tissue models typically characterise dispersive tissue properties in the form of Debye, Lorenz or Cole-Cole
43 models. These relations incorporate a series of dispersive poles that have been reported to correspond to different physical
44 processes [11–13]. Dispersions at frequencies in excess of 1 GHz are reported to be due to polarisation of water molecules
45 [11]. Similarly, poles within the range 1 MHz to 1 GHz correspond to polarisation of cellular membranes. Low frequency
46 (below 1 MHz) dispersions have been reported to correspond to ionic diffusion processes across the cell membrane [11].
47 Where simulation studies of the electric field have incorporated dispersive tissue properties, all dispersive poles for each
48 biological tissue have been included [2, 7]. As a result, the functional influence that individual dispersive poles and their
49 corresponding physical processes exert on the efficacy of a given stimulus remains unknown.

50 Models which incorporated tissue capacitance, including those incorporating dispersion, have predominantly em-
51 ployed frequency-domain solution methods [2, 6, 7]. Incorporating a greater number of dispersive poles in frequency-
52 domain solutions carries minimal additional memory storage requirements. However time-domain solutions require a
53 linear increase in memory requirements corresponding to the addition of each dispersive poles [15]. Therefore, the ability
54 to identify dispersive poles that do not functionally affect the predicted outcome of stimulation may be advantageous
55 when attempting to simplify dispersive tissue models.

56 Furthermore, analysis of the contribution of the different dispersive regions in the electrical conductivity and per-
57 mittivity of biological tissues can provide insight into the physiological and physical processes that influence electrical

58 stimulation of neural tissue. While it may intuitively be expected that the contribution of high frequency poles lying
 59 outside the frequency range of interest for stimulation will be negligible, it is possible that in the Debye, Lorenz or Cole-
 60 Cole formulation, neglect of individual poles may effect the distribution of conductivity and permittivity values at lower
 61 frequencies which may influence the distribution of the electric field during stimulation. Additionally, it is not known how
 62 low-frequency dielectric dispersions individually alter the electric field and subsequent thresholds for stimulation.

63 To address this, the aim of the present study was to quantify the effects of individual dispersive poles on the output
 64 waveform in the vicinity of the stimulating electrode and on the threshold for activation of a generalized mammalian axon
 65 in brain and muscle tissue.

66 2 Methods

67 Electrical stimuli were synthesised based on typical stimulation parameters for brain and muscle tissue. Using an ana-
 68 lytical volume conductor model incorporating full dispersive tissue properties, the voltage waveform was determined at
 69 all nodes of a simulated mammalian axon model lying close to the electrode [16]. The effect of removing subsets of the
 70 available dispersive poles on the voltage waveform and minimum required stimulus amplitude for activation of the axonal
 71 fiber was then quantified.

72 2.1 Stimulus generation

73 Rectangular cathodic stimulus pulses were synthesised in the time-domain for a given pulse repetition frequency, f_p , and
 74 pulse duration, τ_p , using 2000 terms of the trigonometric Fourier series. The Gibb's phenomenon was minimised by
 75 application of the Lanczos sigma approximation [17]. Stimulus parameters were chosen based on values typically used
 76 during deep brain stimulation [18] and neuromuscular electrical stimulation [19], Table 1. Samples were generated at
 77 frequency of $f_s=1$ MHz, which satisfied the Nyquist criterion for all tissues.

78 [Insert Table 1 here.]

79 2.2 Tissue properties

The complex permittivity, $\hat{\epsilon}$, of each biological tissue as a function of the angular frequency, ω , was determined using the
 Cole-Cole equation

$$\hat{\epsilon}(\omega) = \epsilon_{\infty} + \sum_n \frac{\Delta\epsilon_n}{1 + (\frac{j\omega}{f_n})^{(1-\alpha_n)}} + \frac{\sigma_i}{j\omega\epsilon_0} \quad (1)$$

80 The behaviour of a given material is governed by the permittivity at infinity, ϵ_{∞} , and the intrinsic conductivity, σ_i , at
 81 excitation frequencies of infinity and zero respectively. Each individual dispersive pole, n , contributed an incremental
 82 complex relative permittivity, $\Delta\epsilon_n$, at the pole frequency, f_n , which was spread by the parameter, α_n . The Cole-Cole
 83 equation was applied to Debye materials by setting the α term to zero.

84 Brain tissue properties were estimated using the four-pole grey and white matter Cole-Cole models reported by [11],
 85 where each tissue model contained four dispersions, Table 2. Muscle tissue models were determined using the five-pole
 86 anisotropic model presented by [12].

87 [Insert Table 2 here.]

88 2.3 Volume conductor model

An analytical homogeneous volume conductor of infinite extent was simulated, incorporating either isotropic brain tissue or anisotropic muscle tissue. Stimulation was delivered by a point source electrode [20], which injected a current I_S . The transfer function, H , which calculates the voltage at a distance r from a unit input point current source within a medium having radial and longitudinal conductivities, $\hat{\sigma}_r$ and $\hat{\sigma}_z$ respectively, as a function of frequency was given by

$$H(r, z, \omega) = \frac{1}{4\pi\hat{\sigma}_r(\omega)\sqrt{r^2\frac{\hat{\sigma}_z(\omega)}{\hat{\sigma}_r(\omega)} + z^2}} \quad (2)$$

The periodic voltage waveform, y , in the tissue at a point at a distance r from the stimulating electrode injecting current $x(t)$ was calculated using the Fourier transform, \mathcal{F}

$$y(r, z, t) = \mathcal{F}^{-1} \left[H(r, z, \omega) \cdot \mathcal{F}(x(t)) \right] \quad (3)$$

89 Volume conductor simulations were implemented in Python using the SciPy FFT library [21].

90 2.4 Quantification of errors

91 For each biological tissue, dispersions were removed in order of highest to lowest frequency. As n dispersive poles
 92 were removed, the voltage waveform, $y_n(t)$, at a given distance from the injected current was simulated. The error, E_n ,
 93 compared to the voltage waveform, $y_0(t)$, incorporating all dispersions was calculated within the interval spanning the
 94 rising edge of the pulse at t_0 to the falling edge of the pulse at $t_0 + \tau_p$ as follows

$$E_n = \sqrt{\int_{t=t_0}^{t=t_0+\tau_p} \left(\frac{y_n(t) - y_0(t)}{y_0(t)} \right)^2 dt} \quad (4)$$

95 2.5 Calculation of neural activation thresholds

96 The effect of removing individual dispersive poles on the minimum stimulation amplitudes required to elicit action po-
 97 tential propagation was quantified using the myelinated mammalian axon model developed by McIntyre *et al.* [22]. Each
 98 axon included 21 nodes of ranvier, spaced at 500.0 μm intervals. The fiber diameter was set to 5.7 μm , and all diameter-
 99 dependent parameter values were set according to those reported in [22].

100 The multicompartment axon model was implemented in NEURON 7.3 in conjunction with the Python interpreter [23].

101 The voltage at each nodal and internodal compartment was calculated and applied as an extracellular potential. Numerical
102 integration was performed using the Crank-Nicholson method using a time step of $1\ \mu\text{s}$. The Brent optimisation method,
103 as implemented by the SciPy package [21], was used to determine the minimum stimulus current required to elicit action
104 potential propagation in a myelinated axon located 5 mm from the stimulation point, to a tolerance of 1 pA.

105 Pulse durations were varied from $50.0\ \mu\text{s}$ to $400.0\ \mu\text{s}$ in the case of brain tissue, and from $100.0\ \mu\text{s}$ to 1 ms in the case
106 of muscle tissue. Simulations were conducted in parallel using the message-passing interface following the bulletin-board
107 worker model [24]. Postprocessing was carried out using custom written Python 2.7 code.

108 2.6 Analysis of low-frequency poles

109 To examine the effects of the low-frequency poles, the n highest-frequency poles for which the errors were less than 0.1
110 were removed. For the materials examined, the highest two poles were removed in brain tissue, $n = 2$, and the highest
111 three poles were removed in muscle tissue, $n = 3$. The analysis was then repeated for the remaining subset of poles, with
112 the first, $k = 1$, and second, $k = 2$, poles separately removed, so that their effects on the temporal voltage waveform and
113 threshold stimulation amplitude could be isolated.

114 3 Results

115 3.1 Voltage waveforms in tissue

116 Temporal voltage waveforms for a portion of one stimulation period are presented in Figure 1 for all tissues, for a repre-
117 sentative stimulus pulse of 1 mA amplitude and duration $400\ \mu\text{s}$. Errors following the removal of n poles ($n = 1, 2, \dots, 5$)
118 using Equation 4 are detailed in Table 3.

119 [Insert Figure 1 here.]

120 [Insert Table 3 here.]

121 For all tissues, errors were negligible when poles at frequencies in excess of 100 kHz were removed, E_1 and E_2 in
122 Table 3. In the case of grey matter, removal of the third pole in order of descending frequency caused an error of 6.06
123 which altered slightly the waveform shape Figure 1(a). Removal of the final remaining pole resulted in an error of 44.31
124 and increased the peak magnitude of the voltage waveform by a factor of approximately four.

125 Similar results were observed for white matter, where removal of the third and fourth poles in order of descending
126 frequency, resulted in errors of 3.16 and 11.84 relative to the case where all poles were included. A similar variation in
127 shape to that observed in grey matter was observed, along with a slightly smaller increase in the peak amplitude of the
128 waveform, Figure 1(b).

129 In the case of muscle tissue, removal of the first two poles resulted in negligible errors, whilst the error following the
130 removal of the third pole was 0.05, Table 3. Removal of the fourth pole resulted in a modification of the waveform shape,
131 Figure 1(c), and a corresponding error of 0.67. When the fifth pole was removed, the error increased to 46.65, however
132 the increase in peak magnitude was less than that observed for brain tissues, Figure 1.

133 **3.2 Stimulation thresholds**

134 Stimulation thresholds were determined for brain and muscle tissue, and are presented in Table 4. For brain tissues,
135 the threshold current values for grey matter and white matter were unchanged as the two poles with the highest pole
136 frequencies were removed from the parametric Cole-Cole model. Similarly, for muscle tissues, the required stimulation
137 amplitude remained constant as the first three poles were removed in order of descending pole frequency, $k = \{5, 4, 3\}$.

138 [Insert Table 4 here.]

139 In the case of grey matter, the required stimulation amplitude was reduced by 14.7 % when the pole $k = 2$ at 1.5 kHz
140 was removed. When the pole $k = 1$ at 30 Hz was additionally removed, the stimulation amplitude was reduced by 85 %
141 relative to the case when all poles were included.

142 For white matter, removal of the pole $k = 2$ at 3.0 kHz resulted in a small reduction of 3.4 % in the required stimulation
143 amplitude to 83 μ A. Removal of final remaining pole $k = 1$ at 20 Hz resulted in a reduction of 70.1 % in the required
144 stimulation amplitude relative to the case where all poles were included. In the case of muscle tissues, removal of the pole
145 $k = 2$ at 38 kHz reduced the required stimulation amplitude by 3.9 %, and removal of the final remaining pole at 150 Hz
146 resulted in a reduction of 33.8 % in the required stimulation amplitude relative to the case where all poles were included.

147 The minimum amplitudes for stimulation were then examined as pulse durations were varied, Figure 2. The results
148 remained consistent with the relative differences presented in Table 4 as pulse durations were varied from 50.0 μ s to
149 400.0 μ s for brain tissue, Figure 2(a) and Figure 2(b), and from 100.0 μ s to 1 ms for muscle tissue, Figure 2(c).

150 [Insert Figure 2 here.]

151 **3.3 Individual effects of low-frequency poles**

152 As removal of the poles at frequencies above 100 kHz resulted in negligible errors for all tissues, the effects of the two
153 lowest-frequency poles were then individually examined, Figure 3. All poles were removed and the effect of incorporating
154 each of the two lowest frequency poles on the voltage waveform was estimated Figure 4. Corresponding errors, with
155 respect to the full dispersive solution, and threshold stimulus amplitudes when each of the low frequency poles were
156 individually removed are presented in Table 5.

157 [Insert Figure 3 here.]

158 [Insert Figure 4 here.]

159 [Insert Table 5 here.]

160 [Insert Figure 5 here.]

161 For grey and white matter brain tissues, removal of the lowest frequency pole, $k = 1$, increased the peak amplitude of
162 the waveform, reducing the threshold stimulus amplitudes by 74.8 % and 66.7 % for grey and white matter respectively. A
163 similar result was observed for muscle tissue, although the change in amplitude was of a smaller magnitude, Figure 4(c).

164 Similarly, the reduction in required stimulation amplitude of 31.8 % was less than that for brain tissues. The relative effect
165 of removing the two low-frequency poles remained consistent with the results presented in Table 5 as pulse durations were
166 varied from 50.0 μ s to 400.0 μ s for brain tissue, Figure 5(a) and Figure 5(b), and from 100.0 μ s to 1 ms for muscle tissue,
167 Figure 5(c).

168 4 Discussion

169 The aim of this study was to quantify the effect of using a subset of the available dispersive poles to describe the frequency-
170 dependent electrical properties of brain and muscle tissue when estimating threshold amplitudes for neural stimulation.
171 The results provide guidance on simplifying parametric models for dielectric tissues in computational studies of neural
172 stimulation through the removal of high frequency poles. In addition, the specific effects of the remaining low-frequency
173 poles were quantified.

174 For all tissues examined, errors in the voltage waveform were less than 0.05 when poles at frequencies in excess of
175 100 kHz were neglected, Table 3. Similarly, changes to threshold stimulation amplitudes were found to be negligible as
176 poles at frequencies in excess of 100 kHz, reported to correspond to polarisation of cell membranes and water molecules
177 [11], were removed, Table 4. These results confirm that when constructing volume conductor models for investigating
178 the neural response to typically applied electrical stimuli in brain and muscle tissues, poles in excess of 100 kHz may be
179 neglected.

180 The effects of the remaining two low-frequency poles, associated with diffusion processes at cell membranes [11],
181 were then examined separately. Removal of the lowest-frequency pole, situated within the frequency range 0 Hz to 1 kHz,
182 caused an increase in the peak amplitude of the temporal voltage waveform, Figure 4. This resulted in a consequential
183 reduction in the minimum stimulus amplitude required to elicit neural activation, a_1 , compared to that prior to removal,
184 a_0 , Table 5. A smaller, though still pronounced, effect was observed in muscle tissue compared to brain tissue. These
185 observations indicate that poles at frequencies below 1 kHz primarily influence the magnitude of the voltage waveform,
186 and therefore have a considerable effect on stimulus amplitudes required to elicit axonal activation. This can be seen also
187 from the resulting distribution of the conductivity and relative permittivity, Figure 3 (a,b,c) where a substantial decrease
188 in the tissue conductivity at frequencies greater than 10 Hz is observed when the lowest pole is removed, particularly in
189 grey and white matter brain tissue.

190 The effect of removing poles within the range 1 kHz to 100 kHz was then examined, and was found to primarily affect
191 the shape of the waveform with a negligible change in its peak magnitude for all tissues, Figure 4. This corresponded to
192 small changes in the required stimulation amplitude necessary to elicit neural activation, a_2 , compared to that required
193 prior to the pole's removal, a_0 , Table 5. The significance of this effect will depend on the precise neuron model used to
194 determine the efficacy of the stimulus. This effect may be understood by considering the effect of removing the second
195 pole on the conductivity and relative permittivity, Figure 3 (d,e,f) where the effect of removing the second pole is greatest
196 on the relative permittivity at frequencies above approximately 100 Hz.

197 Although the results and conclusions drawn are likely to be of greatest benefit to models utilising time-domain solvers,

198 the analysis was done in the frequency domain to ensure computational uniformity across all simulations. The majority
199 of published computational studies in the area of brain and muscle stimulation have employed similar frequency-domain
200 approaches to that utilized in this work [2, 6–8]. Dispersive media are easily simulated in this way, either in analytical
201 point current-source models, or in finite element method applications that discretize the time-harmonic Laplace equation.
202 Assuming a linear electrical tissue model, superposition permits dispersive frequency-dependent parametric tissue models
203 to be utilised in place of fixed conductivities and permittivities. The frequency-domain approach imposes a number of
204 limitations, and is most suited to periodic pulse waveforms where the stimulation parameters, other than amplitude, are
205 fixed prior to simulation. However, several suggested stimulation paradigms involve the synthesis of arbitrary waveforms,
206 the characteristics of which are not known a priori [25, 26], and simulation of these approaches may be more suited to
207 time-domain solution. Similarly, the simulation of closed-loop stimulation paradigms in which the frequency, waveform
208 shape or duration of the stimulus pulse change as a function of time may be better approached using time-domain solvers.
209 The results observed in this study have the potential to reduce the memory storage requirements for the tissues studied by
210 up to 75 % in time-domain simulations [15], which may improve the computational tractability of simulations involving
211 time-varying or aperiodic stimuli.

212 This study was carried out subject to a number of limitations, which should be considered when interpreting the results
213 and conclusions. The volume conductor was simulated using an analytical point current source model, as used in other
214 field-neuron models [2, 16]. This approach neglected the effects of several electromagnetic features such as the electrode-
215 tissue interface [27], encapsulation tissue surrounding the stimulation electrode [28], tissue anisotropy [29], reference
216 electrode [30] and more complex stimulation electrode geometries [7, 31]. The overall findings of this study, however,
217 should hold in the presence of more complex geometries though the exact values of the errors observed will vary according
218 to the specifics of each model. The analysis has been confined to the frequency range where inductive and propagation
219 effects are negligible, which is the case for the frequencies of interest during electrical neural stimulation [1, 2]. The
220 parametric models used to characterize the electrical properties of the biological tissues are based on experimental studies
221 and individual parameters are subject to uncertainties [32], which have been shown to be capable of altering the resulting
222 shape and extent of the region of neural tissue activated [33]. Cole-Cole parametric models were available for brain
223 tissues [11], however, only Debye parameterizations were available for muscle tissues [12]. Measurements *in-vivo* exhibit
224 a slightly greater frequency response in the conductivity and differences in the magnitude and frequency response of the
225 relative permittivity, related to the different responses of lower and higher frequency dispersions following cell death [34].

226 **5 Conclusion**

227 The effect of individual poles in the dielectric dispersion of brain and muscle tissue on the volume conducted voltage
228 waveform and thresholds for nerve electrical stimulation were examined using model simulation. Removal of poles
229 below 100 kHz resulted in errors in the voltage waveform and, consequentially, in the minimum stimulus amplitudes
230 necessary to elicit axonal activation. For all tissues, poles at frequencies between zero and 1 kHz primarily influenced
231 the voltage waveform's magnitude, and had the greatest effect on predicted minimum stimulation amplitudes. Poles at

232 frequencies from 1 kHz to 100 kHz influenced the voltage waveforms shape, and had a relatively minor effect on required
233 minimum stimulus amplitudes. The results support the simplification of classic models of dielectric dispersion under
234 these conditions. These simplifications would be of particular benefit in the design of time-domain numerical solvers for
235 simulating time-varying stimulation as may occur, for example, in closed-loop stimulation paradigms.

236 **Acknowledgments**

- 237 1. This work is supported in part by ERC Consolidator Grant ERC-2014-CoG 646923 DBSModel.
- 238 2. The authors acknowledge the Research IT Service at University College Dublin ([http://www.ucd.ie/itservices/](http://www.ucd.ie/itservices/researchit/)
239 [researchit/](http://www.ucd.ie/itservices/researchit/)) and the Irish Centre for High-End Computing for providing HPC resources that have contributed to
240 the research results reported within this paper.

241 **References**

- 242 [1] R. Plonsey, D. B. Heppner, Considerations of quasi-stationarity in electrophysiological systems., *Bull Math Biophys*
243 29 (4) (1967) 657–664.
- 244 [2] C. A. Bossetti, M. J. Birdno, W. M. Grill, Analysis of the quasi-static approximation for calculating potentials
245 generated by neural stimulation., *J Neural Eng* 5 (1) (2008) 44–53.
- 246 [3] L. Mesin, R. Merletti, Distribution of electrical stimulation current in a planar multilayer anisotropic tissue., *IEEE*
247 *Trans Biomed Eng* 55 (2 Pt 1) (2008) 660–670.
- 248 [4] N. S. Stoykov, M. M. Lowery, A. Taflove, T. A. Kuiken, Frequency- and time-domain fem models of EMG: capaci-
249 tive effects and aspects of dispersion., *IEEE Trans Biomed Eng* 49 (8) (2002) 763–772.
- 250 [5] M. M. Lowery, N. S. Stoykov, J. P. A. Dewald, T. A. Kuiken, Volume conduction in an anatomically based surface
251 EMG model., *IEEE Trans Biomed Eng* 51 (12) (2004) 2138–2147.
- 252 [6] C. R. Butson, C. C. McIntyre, Tissue and electrode capacitance reduce neural activation volumes during deep brain
253 stimulation., *Clin Neurophysiol* 116 (10) (2005) 2490–2500.
- 254 [7] P. F. Grant, M. M. Lowery, Effect of dispersive conductivity and permittivity in volume conductor models of deep
255 brain stimulation, *IEEE Trans Biomed Eng* 57 (10) (2010) 2386–2393. doi:10.1109/TBME.2010.2055054.
- 256 [8] N. Yousif, X. Liu, Investigating the depth electrode-brain interface in deep brain stimulation using finite element
257 models with graded complexity in structure and solution., *J Neurosci Methods*.
- 258 [9] C. Gabriel, S. Gabriel, E. Corthout, The dielectric properties of biological tissues: I. literature survey., *Phys Med*
259 *Biol* 41 (11) (1996) 2231–2249.

- 260 [10] S. Gabriel, R. W. Lau, C. Gabriel, The dielectric properties of biological tissues: II. measurements in the frequency
261 range 10 hz to 20 ghz., *Phys Med Biol* 41 (11) (1996) 2251–2269.
- 262 [11] S. Gabriel, R. W. Lau, C. Gabriel, The dielectric properties of biological tissues: III. parametric models for the
263 dielectric spectrum of tissues., *Phys Med Biol* 41 (11) (1996) 2271–2293.
- 264 [12] W. D. Hurt, Multiterm debye dispersion relations for permittivity of muscle, *IEEE Trans Biomed Eng* 32 (1) (1985)
265 60–4.
- 266 [13] N. K. Logothetis, C. Kayser, A. Oeltermann, In vivo measurement of cortical impedance spectrum in monkeys:
267 implications for signal propagation, *Neuron* 55 (5) (2007) 809–23.
- 268 [14] B. Tracey, M. Williams, Computationally efficient bioelectric field modeling and effects of frequency-dependent
269 tissue capacitance, *J Neural Eng* 8 (3) (2011) 036017.
- 270 [15] N. S. Stoykov, T. A. Kuiken, M. M. Lowery, A. Taflove, Finite-element time-domain algorithms for modeling linear
271 debye and lorentz dielectric dispersions at low frequencies., *IEEE Trans Biomed Eng* 50 (9) (2003) 1100–1107.
- 272 [16] P. F. Grant, M. M. Lowery, Contribution of dielectric dispersions to voltage waveforms arising from electrical stim-
273 ulation, in: *Proceedings of the 34th International IEEE Engineering in Medicine and Biology Conference, 2012*, pp.
274 4148–4151. doi : 10.1109/EMBC.2012.6346880.
- 275 [17] A. J. Jerri, *The Gibbs Phenomenon in Fourier Analysis, Splines and Wavelet Approximations*, Kluwer Academic
276 Publishers, 1998.
- 277 [18] J. Volkmann, J. Herzog, F. Kopper, G. Deuschl, Introduction to the programming of deep brain stimulators., *Mov*
278 *Disord* 17 Suppl 3 (2002) S181–7.
- 279 [19] B. M. Doucet, A. Lam, L. Griffin, Neuromuscular electrical stimulation for skeletal muscle function, *Yale J Biol*
280 *Med* 85 (2) (2012) 201–15.
- 281 [20] C. C. McIntyre, W. M. Grill, Finite element analysis of the current-density and electric field generated by metal
282 microelectrodes., *Ann Biomed Eng* 29 (3) (2001) 227–235.
- 283 [21] E. Jones, T. Oliphant, P. Peterson, et al., *SciPy: Open source scientific tools for Python* (2001).
- 284 [22] C. C. McIntyre, A. G. Richardson, W. M. Grill, Modeling the excitability of mammalian nerve fibers: influence of
285 afterpotentials on the recovery cycle., *J Neurophysiol* 87 (2) (2002) 995–1006.
- 286 [23] M. L. Hines, N. T. Carnevale, The NEURON simulation environment, *Neural Comput* 9 (6) (1997) 1179–209.
- 287 [24] M. L. Hines, N. T. Carnevale, Translating network models to parallel hardware in NEURON, *J Neurosci Methods*
288 169 (2) (2008) 425–55.
- 289 [25] O. Popovych, C. Hauptmann, P. Tass, Demand-controlled desynchronization of brain rhythms by means of nonlinear
290 delayed feedback., *Conf Proc IEEE Eng Med Biol Soc* 7 (2005) 7656–7659.

- 291 [26] C. Hauptmann, P. A. Tass, Therapeutic rewiring by means of desynchronizing brain stimulation., *Biosystems* 89 (1-
292 3) (2007) 173–181.
- 293 [27] D. R. Cantrell, S. Inayat, A. Taflove, R. S. Ruoff, J. B. Troy, Incorporation of the electrode-electrolyte interface into
294 finite-element models of metal microelectrodes., *J Neural Eng* 5 (1) (2008) 54–67.
- 295 [28] W. M. Grill, J. T. Mortimer, Electrical properties of implant encapsulation tissue., *Ann Biomed Eng* 22 (1) (1994)
296 23–33.
- 297 [29] C. C. McIntyre, S. Mori, D. L. Sherman, N. V. Thakor, J. L. Vitek, Electric field and stimulating influence generated
298 by deep brain stimulation of the subthalamic nucleus., *Clin Neurophysiol* 115 (3) (2004) 589–595.
- 299 [30] P. F. Grant, M. M. Lowery, Electric field distribution in a finite-volume head model of deep brain stimulation, *Med*
300 *Eng Phys* 31 (9) (2009) 1095–103. doi : 10 . 1016 / j . medengphy . 2009 . 07 . 006.
- 301 [31] C. Butson, C. McIntyre, Current steering to control the volume of tissue activated during deep brain stimulation.,
302 *Brain Stimulat* 1 (1) (2008) 7–15.
- 303 [32] C. Gabriel, A. Peyman, E. H. Grant, Electrical conductivity of tissue at frequencies below 1 mhz, *Phys Med Biol*
304 54 (16) (2009) 4863–78. doi : 10 . 1088 / 0031 - 9155 / 54 / 16 / 002.
- 305 [33] C. Schmidt, P. Grant, M. Lowery, U. van Rienen, Influence of uncertainties in the material properties of brain tissue
306 on the probabilistic volume of tissue activated, *IEEE Trans Biomed Eng* 60 (5) (2013) 1378–87. doi : 10 . 1109 /
307 *TBME* . 2012 . 2235835.
- 308 [34] T. Wagner, U. Eden, J. Rushmore, C. J. Russo, L. Dipietro, F. Fregni, S. Simon, S. Rotman, N. B. Pitskel, C. Ramos-
309 Estebanez, A. Pascual-Leone, A. J. Grodzinsky, M. Zahn, A. Valero-Cabré, Impact of brain tissue filtering on neu-
310 rostimulation fields: a modeling study, *Neuroimage* 85 Pt 3 (2014) 1048–57. doi : 10 . 1016 / j . neuroimage . 2013 .
311 06 . 079.

312 **List of Figures**

313 1 Voltage waveforms 5 mm from the stimulating electrode in (a) grey matter, (b) white matter and (c) muscle
 314 due to stimulus of 1 mA amplitude and 400.0 μ s duration. For each material, n denotes the number of poles
 315 removed in order of descending frequency. For brain tissues, (a) and (b), as the error was negligible when
 316 the two highest poles were removed, the waveforms are omitted from the plots for reasons of clarity. In
 317 the case of muscle tissue, the cases of $n = 0, 1, 2$ poles removed are similarly omitted, (c). 13

318 2 Threshold current for stimulation, a_n , plotted with respect to stimulation pulse duration. n is the number
 319 of poles removed, in order of descending frequency. For brain tissues, (a) and (b), as the error when one
 320 pole was removed, $k = 1$, was negligible, the waveforms are omitted from the plots for clarity. In the case
 321 of muscle tissue, (c), the cases of $n = 0, 1, 2$ poles removed are similarly omitted. 14

322 3 Relative permittivity and electrical conductivity of (a,d) grey matter, (b,e) white matter and (c,f) muscle
 323 where the lowest, $k = 0$, pole was removed (a,b,c) and where the subsequent, $k = 1$, pole was removed
 324 (d,e,f). Dotted lines show comparison to the case where all poles are incorporated. 15

325 4 Voltage waveforms in (a) grey matter, (b) white matter and (c) due to 1 mA stimulus. For brain tissues, (a)
 326 and (b), the highest two poles are removed. For muscle, (c), the highest three poles are removed. Figures
 327 show the voltage waveform when the lowest two poles, $k = \{1, 2\}$ are separately removed, compared to
 328 the case where no additional poles are removed. 16

329 5 Stimulation threshold, a_n , plotted with respect to stimulation pulse duration. n is the number of poles
 330 removed, in order of descending frequency. For brain tissues, (a) and (b), as the error when no poles
 331 were removed and one pole was removed, $k = 1$, were both negligible, the waveforms are omitted from
 332 the plots for reasons of clarity. In the case of muscle tissue, the cases of $n = 0, 1, 2$ poles removed are
 333 similarly omitted, (c). 17

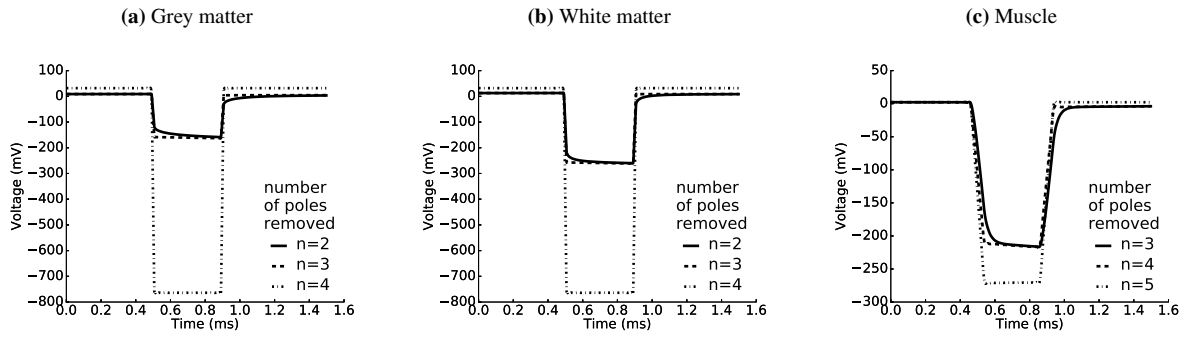


Figure 1: Voltage waveforms 5 mm from the stimulating electrode in (a) grey matter, (b) white matter and (c) muscle due to stimulus of 1 mA amplitude and 400.0 μ s duration. For each material, n denotes the number of poles removed in order of descending frequency. For brain tissues, (a) and (b), as the error was negligible when the two highest poles were removed, the waveforms are omitted from the plots for reasons of clarity. In the case of muscle tissue, the cases of $n = 0, 1, 2$ poles removed are similarly omitted, (c).

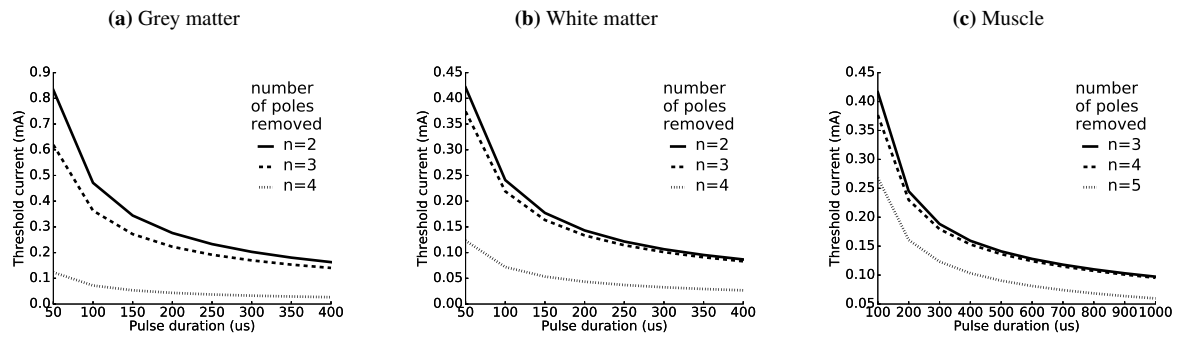


Figure 2: Threshold current for stimulation, a_n , plotted with respect to stimulation pulse duration. n is the number of poles removed, in order of poles descending frequency. For brain tissues, (a) and (b), as the error when one pole was removed, $k = 1$, was negligible, the waveforms are omitted from the plots for clarity. In the case of muscle tissue, (c), the cases of $n = 0, 1, 2$ poles removed are similarly omitted.

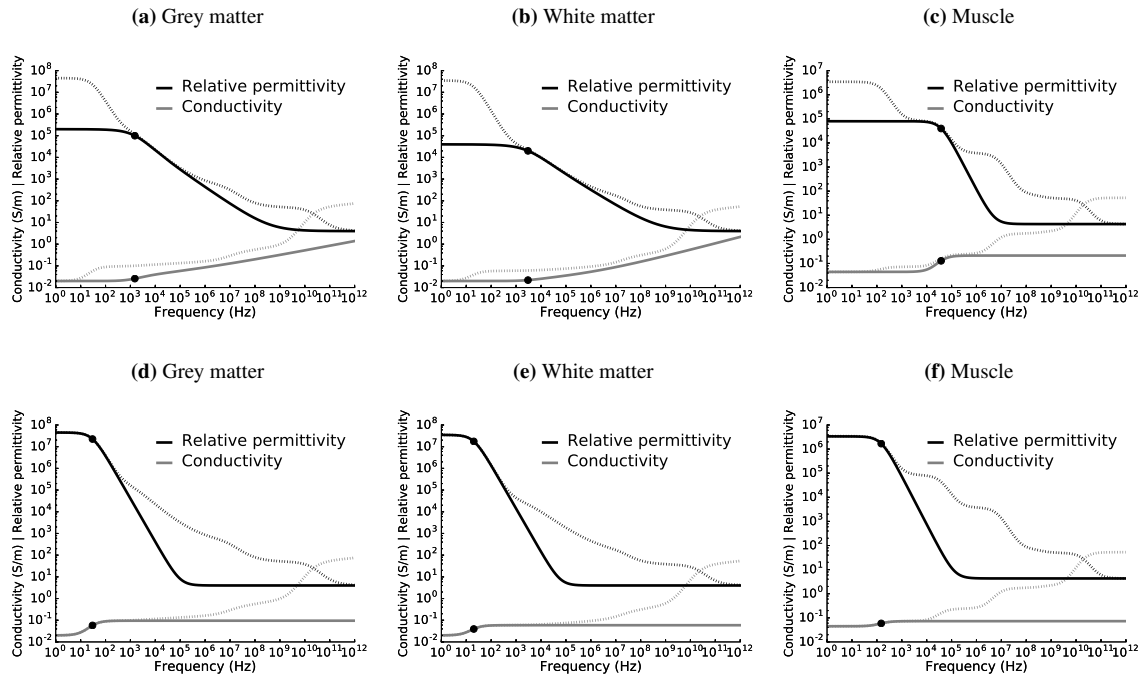


Figure 3: Relative permittivity and electrical conductivity of (a,d) grey matter, (b,e) white matter and (c,f) muscle where the lowest, $k = 0$, pole was removed (a,b,c) and where the subsequent, $k = 1$, pole was removed (d,e,f). Dotted lines show comparison to the case where all poles are incorporated.

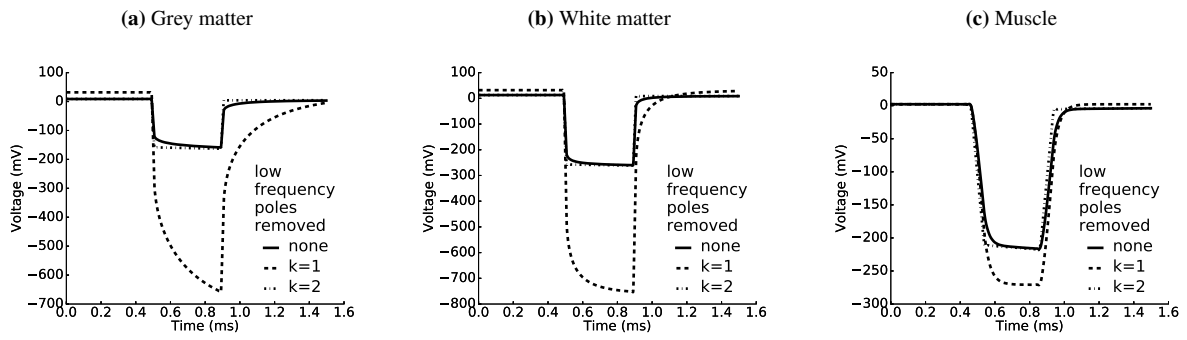


Figure 4: Voltage waveforms in (a) grey matter, (b) white matter and (c) due to 1 mA stimulus. For brain tissues, (a) and (b), the highest two poles are removed. For muscle, (c), the highest three poles are removed. Figures show the voltage waveform when the lowest two poles, $k = \{1, 2\}$ are separately removed, compared to the case where no additional poles are removed.

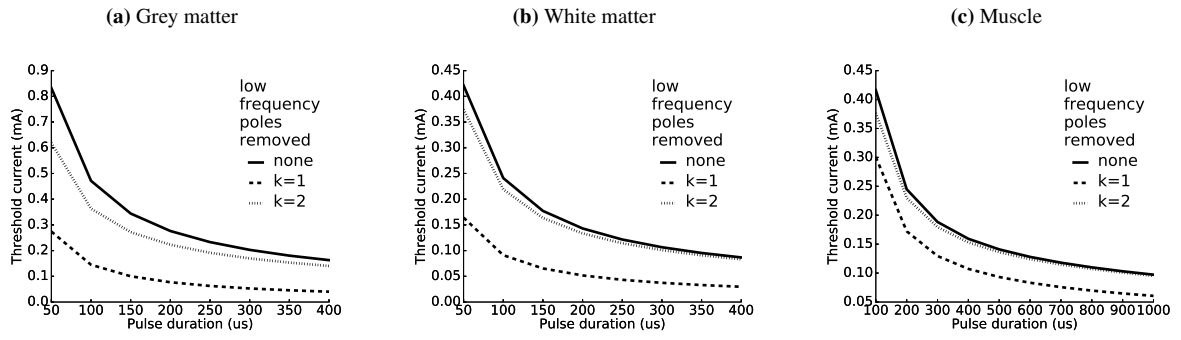


Figure 5: Stimulation threshold, a_n , plotted with respect to stimulation pulse duration. n is the number of poles removed, in order of descending frequency. For brain tissues, (a) and (b), as the error when no poles were removed and one pole was removed, $k = 1$, were both negligible, the waveforms are omitted from the plots for reasons of clarity. In the case of muscle tissue, the cases of $n = 0, 1, 2$ poles removed are similarly omitted, (c).

334 **List of Tables**

335 1 Stimulus parameters for brain tissue and muscle tissue 19

336 2 Parameters values used for Cole-Cole and Debye tissue models to calculate electrical properties. Each
 337 material is defined by ϵ_∞ , the relative permittivity at infinity, and σ_i , intrinsic conductivity. Each pole, k ,
 338 contributes a change in relative permittivity, $\Delta\epsilon_k$, at the pole frequency, f_k , spread by the parameter α_k
 339 in the case of Cole-Cole models. For Debye models, α_k is zero for all k . Brain tissue models have four
 340 poles, muscle tissue model has five poles [11, 12]. 20

341 3 Error, E_n , of the voltage waveform at a distance of 5 mm following the removal of n poles in order of
 342 descending frequency. Values are presented for pulse durations of 400 μ s. 21

343 4 Stimulation current amplitude, a_n , in μ A required to elicit axonal activation at a distance of 5 mm from
 344 the stimulus point current source. n is the number of poles removed, in order of descending frequency. 22

345 5 Error, E_k , of the voltage waveform and stimulation current amplitude, a_k , required to elicit axonal activa-
 346 tion at a distance of 5 mm from the stimulus point current source for an axon located in a homogeneous
 347 medium following the removal of the k th lowest-frequency pole. For comparison, the a_0 case giving the
 348 threshold stimulus amplitude where no poles were removed is also presented. 23

Table 1: Stimulus parameters for brain tissue and muscle tissue

Parameter		Brain Tissue	Muscle Tissue
Repetition frequency	f_p	100 Hz	20 Hz
Pulse duration	τ_p	min	50.0 μ s
		default	400.0 μ s
		max	400.0 μ s

Table 2: Parameters values used for Cole-Cole and Debye tissue models to calculate electrical properties. Each material is defined by ϵ_∞ , the relative permittivity at infinity, and σ_i , intrinsic conductivity. Each pole, k , contributes a change in relative permittivity, $\Delta\epsilon_k$, at the pole frequency, f_k , spread by the parameter α_k in the case of Cole-Cole models. For Debye models, α_k is zero for all k . Brain tissue models have four poles, muscle tissue model has five poles [11, 12].

Material	Component	Ref	ϵ_∞	σ_i	Pole	$k = 1$	$k = 2$	$k = 3$	$k = 4$	$k = 5$
Brain (grey matter)	Isotropic	[11]	4.0	0.02	f_k	30.0 Hz	1.5 kHz	10.0 MHz	20.0 GHz	
					$\Delta\epsilon_k$	4.50×10^7	2.00×10^5	4.00×10^2	4.50×10^1	
					α_k	0.0	0.22	0.15	0.1	
Brain (white matter)	Isotropic	[11]	4.0	0.02	f_k	20.0 Hz	3.0 kHz	20.0 MHz	20.0 GHz	
					$\Delta\epsilon_k$	3.50×10^7	4.00×10^4	1.00×10^2	3.20×10^1	
					α_k	0.0	0.3	0.1	0.1	
Muscle	Transverse	[12]	4.3	0.0762	f_k	69.0 Hz	43.0 kHz	670.0 kHz	230.0 MHz	20.0 GHz
					$\Delta\epsilon_k$	2.00×10^5	8.19×10^4	1.19×10^4	3.20×10^1	4.58×10^1
					α_k	0.0	0.0	0.0	0.0	0.0
Muscle	Parallel	[12]	4.3	0.0446	f_k	150.0 Hz	38.0 kHz	7.3 MHz	370.0 MHz	20.0 GHz
					$\Delta\epsilon_k$	3.37×10^6	7.95×10^4	3.68×10^3	2.00×10^1	4.56×10^1
					α_k	0.0	0.0	0.0	0.0	0.0

Table 3: Error, E_n , of the voltage waveform at a distance of 5 mm following the removal of n poles in order of descending frequency. Values are presented for pulse durations of 400 μ s.

Material	E_1	E_2	E_3	E_4	E_5
Brain (grey matter)	0.00	0.01	6.06	44.31	
Brain (white matter)	0.00	0.00	3.16	11.84	
Muscle	0.00	0.00	0.05	0.67	46.65

Table 4: Stimulation current amplitude, a_n , in μA required to elicit axonal activation at a distance of 5 mm from the stimulus point current source. n is the number of poles removed, in order of descending frequency.

Material	a_0	a_1	a_2	a_3	a_4	a_5
Brain (grey matter)	163	163	163	140	27	
Brain (white matter)	87	87	87	83	27	
Muscle	160	160	160	159	153	103

Table 5: Error, E_k , of the voltage waveform and stimulation current amplitude, a_k , required to elicit axonal activation at a distance of 5 mm from the stimulus point current source for an axon located in a homogeneous medium following the removal of the k th lowest-frequency pole. For comparison, the a_0 case giving the threshold stimulus amplitude where no poles were removed is also presented.

Material	n highest-frequency poles removed	Pole 1 removed		Pole 2 removed		
		$a_{k=0}$	$E_{k=1}$	$a_{k=1}$	$E_{k=2}$	$a_{k=2}$
Brain (grey matter)	2	163 μ A	118.63	40 μ A	7.81	140 μ A
Brain (white matter)	2	87 μ A	18.99	30 μ A	3.50	83 μ A
Muscle	3	159 μ A	84.70	107 μ A	1.11	153 μ A